AD-A132 643 A STUDY OF PLASMASPHERIC DENSITY DISTRIBUTIONS FOR DIFFUSIVE EQUILIBRIUM..(U) UTAH STATE UNIV LOGAN CENTER FOR ATMOSPHERIC AND SPACE SCIENC.. W LI ET AL. MAR 83 1/1

UNCLASSIFIED SCIENTIFIC-1 AFGL-TR-83-0088 F/G 4/1 NL

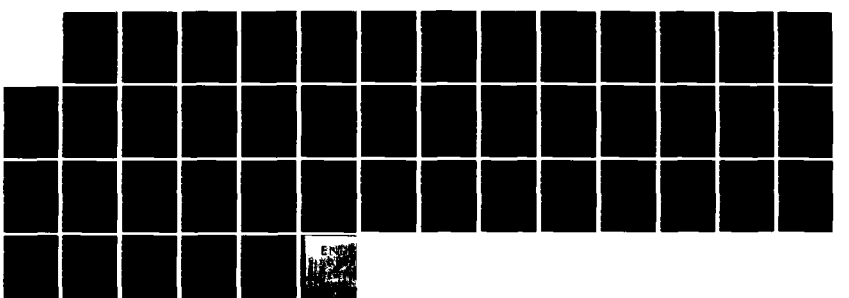

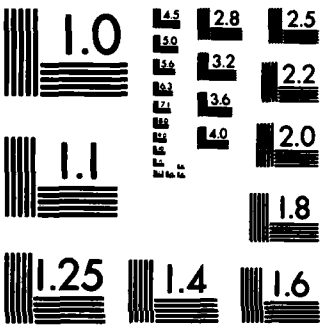

MICROCOPY RESOLUTION TEST CHART
NATIONAL BUREAU OF STANDARDS-1963-A

(12)

AFGL-TR-83-0088

A STUDY OF PLASMASPHERIC DENSITY DISTRIBUTIONS FOR DIFFUSIVE EQUILIBRIUM CONDITIONS

Wenxiu Li
J.J. Sojka
W.J. Raitt

Center for Atmospheric and Space Sciences
Utah State University
Logan, Utah 84322

Scientific Report No. 1

March 1983

AIR FORCE GEOPHYSICS LABORATORY
AIR FORCE SYSTEMS COMMAND
UNITED STATES AIR FORCE
HANSCOM AFB, MASSACHUSETTS 01731

This report has been reviewed by the ESD Public Affairs Office (PA) and is releasable to the National Technical Information Services (NTIS).

This technical report has been reviewed and is approved for publication

Frederick J. Rich

FREDERICK J. RICH
Contract Manager

William J. Burke

WILLIAM J. BURKE, Acting Branch Chf
Plasmas, Paticles & Fields Branch
Space Physics Division

FOR THE COMMANDER

Rita C. Sagalyn

RITA C. SAGALYN, Director
Space Physics Division

Qualified requestors may obtain additional copies from the Defense Technical Information Center. All others should apply to the National Technical Information Service.

If your address has changed, or if you wish to be removed from the mailing list, or if the addressee is no longer employed by your organization, please notify AFGL/DAA, Hanscom AFB, MA 01731. This will assist us in maintaining a current mailing list.

Do not return copies of this report unless contractual obligations or notices on a specific document requires that it be returned.

Unclassified

SECURITY CLASSIFICATION OF THIS PAGE (When Data Entered)

REPORT DOCUMENTATION PAGE		READ INSTRUCTIONS BEFORE COMPLETING FORM
1. REPORT NUMBER AFGL-TR-83-0088	2. GOVT ACCESSION NO. AD A132 643	3. RECIPIENT'S CATALOG NUMBER
4. TITLE (and Subtitle) A STUDY OF PLASMASPHERIC DENSITY DISTRIBUTIONS FOR DIFFUSIVE EQUILIBRIUM CONDITIONS		5. TYPE OF REPORT & PERIOD COVERED Scientific Report No. 1 6. PERFORMING ORG. REPORT NUMBER
7. AUTHOR(s) Wenxiu Li* J.J. Sojka W.J. Raitt		8. CONTRACT OR GRANT NUMBER(s) F19628-83-K-0001
9. PERFORMING ORGANIZATION NAME AND ADDRESS Center for Atmospheric and Space Sciences Utah State University Logan, Utah 84322		10. PROGRAM ELEMENT, PROJECT, TASK AREA & WORK UNIT NUMBERS 61102F 2311G2FD
11. CONTROLLING OFFICE NAME AND ADDRESS Air Force Geophysics Laboratory Hanscom AFB, Massachusetts 01731 Monitor/Frederick J. Rich/PHG		12. REPORT DATE March 1983 13. NUMBER OF PAGES 43
14. MONITORING AGENCY NAME & ADDRESS (if different from Controlling Office)		15. SECURITY CLASS. (of this report) Unclassified 15a. DECLASSIFICATION/DOWNGRADING SCHEDULE

16. DISTRIBUTION STATEMENT (of this Report)

Approved for public release; distribution unlimited

17. DISTRIBUTION STATEMENT (of the abstract entered in Block 20, if different from Report)

18. SUPPLEMENTARY NOTES

*Permanent Address Dept of Earth & Space Sciences
Univ of Science & Technology of China
Hefei, Anhui, People's Republic of China

19. KEY WORDS (Continue on reverse side if necessary and identify by block number)

Ionospheric
Model
Ion density
Electron density
Seasonal variation
Diurnal variation

20. ABSTRACT (Continue on reverse side if necessary and identify by block number)

We have modelled the plasmaspheric density distribution for a range of solar cycle, seasonal and diurnal conditions with a magnetic flux tube dependent diffusion equilibrium model by using experimentally determined values of ionospheric parameters at 675 km as boundary conditions.

Data is presented in terms of plasmaspheric H^+ and He^+ density contours, total flux tube content and equatorial plasma density for a range of L-values from 1.15 to 3.0. The variation of equatorial plasma density for a range of L-values from 1.15 to 3.0. The variation of equatorial density with L-value

DD FORM 1 JAN 73 1473 EDITION OF 1 NOV 65 IS OBSOLETE

Unclassified

SECURITY CLASSIFICATION OF THIS PAGE (When Data Entered)

shows good agreement with the $1/L^4$ dependence observed experimentally.

The results show that the model predicts larger solar cycle and diurnal variation in equatorial plasma density than observed using whistler techniques. However, the whistler method requires a model to deduce the equatorial density and is therefore open to interpretation.

Seasonal variations are rather artificial since in this general model we have not attempted to match equatorial densities for flux tubes emanating from the winter and summer hemispheres.

Introduction

Initial studies of the effects of plasma density gradients on the diffusion dominated regions of the ionosphere concentrated on the application of plasma transport equations to solve for plasma density altitude profiles for the case of the diffusive equilibrium distribution of multi-ion species (cf Mange, 1960). In this case, the pressure gradient existing between the F-region peak and high altitudes results in the ions distributing themselves such that the polarization electric field set up by the pressure gradient is just balanced by the gravitational force on the ions. Under these circumstances the outward flux of ions is zero. When the concept of open or extended geomagnetic field lines became accepted, it was realized that the possibility existed for ions to continuously flow from the earth into the distant regions of the magnetosphere linked by geomagnetic field lines to the polar ionosphere. This condition is one of the solutions of the ion density distribution under diffusion dominated conditions and is known as "dynamic equilibrium" as opposed to "diffusive equilibrium" discussed earlier. Both types of equilibrium represent steady state solutions to the plasma transport equations resulting in the requirement that the outward flux is a constant, zero in the case of diffusive equilibrium and some finite value in the case of dynamic equilibrium (Banks and Kockarts 1973; Bauer, 1973). Boundary conditions on the rate of production of the outflowing ions and Coulomb collisions with stationary ions result in an upper limit to the outward flux. Numerous theoretical models have been developed over the last decade to describe the dynamic equilibrium condition; these models include hydrodynamic models (Banks and Holzer, 1968, 1969a, 1969b; Marubashi, 1970; Banks, 1973; Bailey and Moffett, 1974; Banks et al, 1974, 1976; Strobel and Walker, 1972; Raitt et al, 1975,

1977, 1978a, 1978b; Schunk et al, 1978; Ottley and Schunk, 1980), hydromagnetic models (Holzer et al, 1971), kinetic models (Lemaire and Scherer, 1970, 1971, 1972, 1973; Lemaire, 1972) and models based on generalized transport equations (Schunk and Watkins, 1979, 1981, 1982).

This strong emphasis on the description of the dynamic equilibrium cases has resulted in the diffusive equilibrium case being somewhat neglected since the earlier work referenced above. In particular the extension of model calculations of both the dynamic equilibrium case and the diffusive equilibrium case along a magnetic flux tube all the way from the ionosphere to the equatorial plane has been neglected. Chiu et al (1979) corrected this deficiency for the diffusive equilibrium case by describing a model for plasma density distribution from the ionosphere to the equatorial plane allowing for magnetic flux tube divergence. There is also work being done on more comprehensive models allowing for finite flux values out to the equatorial plane, thus describing inter-hemispheric transport of ionization (Young et al., 1980a, b).

At low latitudes, diffusive equilibrium is assumed to be an adequate description of the plasma density distribution for most local times, and at mid latitudes up to an L-value of about L=3, diffusive equilibrium exists for a smaller fraction of local times; it can, however, be regarded as a limiting case for plasma distribution along flux tubes resulting in a maximum value for the flux tube plasma content. At higher latitudes it is not apparent that diffusive equilibrium ever exists since the flux tubes now approach the plasmapause where the large volume of the flux tube combined with dynamic processes removing plasma at the equatorial plane rarely allow time for diffusive equilibrium to be established. Experimental observations related to the average position of these regions of the plasmasphere have been discussed by

Raitt and Dorling (1976).

It is the purpose of this paper to utilize Chiu's formulation of the plasma density distribution to show how the effects of flux tube divergence can be explicitly allowed for in terms of a dipole magnetic field; and then to use this formulation with experimentally derived boundary conditions to make a parametric study of the plasmaspheric plasma density distribution for the limiting diffusive equilibrium case from L-values of L=1.2 to L=3.0. The range of boundary conditions show marked solar cycle, seasonal and diurnal variations beyond that used by Chiu et al (1979). These dependencies are difficult to reconcile with a diffusive equilibrium model, however by comparing the Chiu model with the results of the more classic flux tube divergence free diffusive equilibrium models it is possible to demonstrate that a diffusive equilibrium formulation is useful for studying the variation of the limiting values of total plasmaspheric content.

Theoretical Model

The computations presented in this study will be based on a hydrodynamic model of the plasma distribution along a flux tube linking the ionosphere to the equatorial plane. Earlier hydrodynamic models referred to above did not account for the divergence of a magnetic flux tube as it was followed away from the lower ionosphere to the equatorial plane. In many cases this omission was not very significant since the plasma distribution was being followed only over a relatively small altitude range compared to the range being studied presently. However, this effect was allowed for by Chiu et al, (1979) in their hydrodynamic formulation by means of a force parallel to B acting on the plasma in the flux tube. In our study we have started from the standard

hydrodynamic continuity and momentum equations for multicomponent plasma and allowed for the flux tube divergence by including its effect in the formulation of the pressure gradient term in the momentum equation.

If we assume that plasma transport occurs only parallel to B, and we identify a spatial coordinate S with distance along a diverging flux tube, we can write the steady state equations of continuity and momentum transport for charged particle species j as:

Continuity:

$$\frac{1}{A(s)} \frac{\partial}{\partial s} [n_j u_j A(s)] = Q_j(s) - L_j(s) \tag{1}$$

where A(s) = area of flux tube at distance S from lower boundary

n_j = number density of species j

u_j = flow speed of species j parallel to B

Q_j = production rate of species j

L_j = loss rate of species j

Momentum:

$$u_j \frac{\partial u_j}{\partial s} + \frac{1}{A(s) n_j m_j} \frac{\partial A(s) P_j}{\partial s} - \left[\frac{q_j E}{m_j} + g(r)\right] \cdot \hat{s} - \Omega_t^2 r \sin\theta \, \hat{e}_c \cdot \hat{s}$$

$$= -\sum_k \nu_{jk} (u_j - u_k) \tag{2}$$

where the additional parameters are:

m_j = mass of species j

P_j = kinetic pressure of species j

q_j = electric charge of species j

E = polarization electric field

$g(r)$ = gravitational acceleration

Ω_t = angular speed of earth's rotation

θ = colatitude of point on flux tube

r = distance from center of earth

$\hat{e}_c$ = unit vector of the centrifugal force

ν_{jk} = collision frequency between species j & k

If we now consider only diffusive equilibrium that is $u_i = u_e = 0$ and use the fact that $B(s)/B(s_o)$ is proportional to $A(s_o)/A(s)$ we obtain the equation for the distribution of plasma density

$$n(s) = n_o\,[B_s\,T_o/B_o\,T_s]\cdot\exp\int_{s_o}^{s} ds'$$

$$[q_e E\cdot\hat{s}' + \tfrac{1}{2}m\Omega_t^2 r\sin 2\theta\,\hat{e}_\theta\cdot\hat{s}' - m(GM_t/r^3 - \Omega_t^2\sin^2\theta)r.\hat{s}']/kT(s') \qquad (3)$$

directly without invoking Chiu's parameter F . Where the additional parameters are:

B_s = geomagnetic field at point s from lower boundary

B_o = geomagnetic field at lower boundary

G = universal gravitational constant

M_t = mass of earth

$\hat{e}_\theta$ = unit vector of the transverse component of the centrifugal force

k = Boltzmann's constant

T = species kinetic temperature

In order to recover the more classical diffusive equilibrium formulation which would not contain flux tube divergence the magnetic field strength ratio B_s/B_o in equation 3 would be set to unity.

Assuming a dipole magnetic field, the electron and ion densities along the flux tube can be given in terms of the colatitude (θ) of the point on the flux tube, in the form

$$n_e(s) = n_{eo} [B_s T_o/B_o T_s] \exp (m_e I)/\exp(\phi) \tag{4}$$

$$n_i(s) = n_{io} [B_s T_o/B_o T_s] \exp (\phi) \exp(m_i I) \tag{5}$$

where the integrals I and ϕ are defined as

$$I = \int_{\theta_o}^{\theta} d\theta' (-2GM_t \cos\theta'/r_o \sin^3\theta' + 3\Omega_t^2 r_o^2 \cos\theta' \sin^5\theta')/kT(\theta') \tag{6}$$

$$\phi = \int_{s_o}^{s} [q_e E \cdot \hat{s}'/kT(s')] ds' \tag{7}$$

Using the neutrality assumption at each point along a flux tube

$$n_e = n_{H^+} + n_{He^+} + n_{O^+} \tag{8}$$

the integral ϕ can be expressed in terms of I as

$$\exp(\phi) = [n_{eo} \exp(m_e I)/\Sigma_i n_{io} \exp(m_i I)]^{1/2} \tag{9}$$

Combining equations (4), (5) and (9) it can be seen that the electron and ion densities depend only upon the integral I the evaluation of which requires a plasma temperature profile along the flux tube. We have adopted the functional form of the temperature used by Chiu et al, (1979) as

$$T(s) = T_o + T_1 ((L-1)/L_o)^{\alpha} (s/\ell)^{\beta} \tag{10}$$

where ℓ is the length of a flux tube from lower boundary to the equator, the constants α and β define the shape of the temperature profile and are discussed later when actual boundary conditions are defined.

The integral I can be evaluated by Simpson's rule for each θ value along a flux tube, the ion densities and integral ϕ can be developed from equations (5) and (9) respectively. In order to get the polarization electric potential Φ from ϕ the differential relation between electric field E and electric potential Φ is used and Φ is expressed in terms of ϕ in the form

$$\Phi = \int_{s_o}^{s} \frac{1}{q_e} ds' [KT(s') \frac{d\phi}{ds'}] \tag{11}$$

which again can be integrated by Simpson rule.

Boundary Conditions

The diffusive equilibrium model, described in the previous section, requires density boundary conditions for all three ion species at the foot of the field line. In addition the full temperature profile from the foot of the field line to the equator is required. For this study, these boundary conditions were determined empirically, based on experimental data. The observations of both ion density and plasma temperature in the region $L < 3$ have shown wide dynamic ranges which have been attributed to solar cycle, seasonal, diurnal and geomagnetic storm effects. Since it is the purpose of this study to test whether diffusive equilibrium can resonably be used to describe the inner plasmasphere our selection of boundary conditions should reflect the changes due to long period mechanisms, for example, boundary condition changes on storm time scales would not be consistent with a diffusive equilibrium model and any agreement with plasmaspheric densities would be purely fortuitous. The selection of boundary conditions will therefore concentrate on reproducing observed solar cycle, seasonal and diurnal variations. It could be argued that diurnal time scales are also too short for diffusive equilibrium to be maintained, however, for the range of L-values studied, we assumed that both day and night ionospheres were in diffusive equilibrium. The problems associated with seasonal effects resulting in the boundary conditions at one foot of a field line differing from its other foot will be addressed in a later section; in our initial study we assumed that the plasma distribution on a field line can be computed for the segment from the ionosphere to the equatorial plane.

1. Ion Density at 675 km.

The choice of an altitude at which to start the diffusive equilibrium model is somewhat arbitrary. Since we intend to model H^+, He^+ and O^+ we need to select an altitude at which measurements of all three ions are available over a range of solar cycle conditions. An altitude of 675 km was selected, and where possible data was used only if it was within about 25 km of this altitude. The relatively small scale heights for the heavy ion species and the plasma temperature variation for the light ions in this altitude range makes extrapolation of densities to other altitudes prone to error. Data from a variety of satellites analyzed by a number of authors were compared and reduced to a single set of values for each solar cycle - season - diurnal combination. Although this range of conditions at 675 km is not completely covered by data in the literature, it is more complete than at other altitudes. To help fill the gaps in the availability of boundary conditions and resolve discrepancies our selection has been biased by the following set of currently accepted physical guidelines:

1) Solar minimum densities at 675 km are lower than at solar maximum.

2) A seasonal anomaly in F-region plasma density exists.

3) Nighttime densities are generally lower than daytime densities.

In searching through the literature examples contradicting these guidelines were found, however, the bulk of the data are consistent with these trends. Table 1 lists the authors and satellites used in obtaining the density boundary conditions. From these measurements the densities shown in Table 2a and 2b were inferred. Many of the entries in Table 2 are described relative to one

particular entry. This is particlarly true for composition and is used to indicate trends. At other times when no particularly significant trend was present, entries are referred to as being the same. From the measurements it was evident that the ionosphere at 675 km could be broken into two regions; a) from L = 1.15 to 1.5 and b) from 1.5 to 3.0. Beyond L = 3.0 effects such as the light ion trough indicate that the description of the plasma distribution of the light ions by diffusive equilibrium is inappropriate. In the inner region, see Table 2a, the boundary conditions are latitude independent (L value) whereas for the outer region, see Table 2b, latitudinal variations are important.

2. Plasma Temperature

The temperature "boundary" conditions requires a full temperature altitude profile for each set of conditions. Such observations are not available, hence a combination of ionospheric and plasmaspheric observations were used to represent extremes of temperature in these different locations and then a set of coefficients for equation 10 were determined such that a reasonable altitude profile of temperature is obtained using equation 10. The validity of equation 10 is tested and discussed in a later section. In order to determine the plasma temperature both the ion and electron temperatures are required. Table 3 lists the authors and satellites from which the temperatures spanning the solar cycle, season and day-night conditions were obtained. These plasma temperatures and their latitudinal variations are given in Tables 4a and 4b. Figure 1 represents several cases of temperature-altitude variation for L = 2. These profiles are representative of the variations contained in Tables 4a and 4b. In each case the plasma temperature at the foot of the field line is lower than that at the equator with temperature increasing relatively rapidly

at low altitudes. Such an altitude shape is consistent with the limited low altitude temperature gradient measurements available and the calculations from more rigorous full flow models (Richards, private communication 1982).

Diffusive Equilibrium Plasmaspheric Densities

The model described above was used to compute the plasma number density distribution along magnetic flux tubes from 675 km to the equator for the field lines described by L = 1.15, 1.5, 2.0, 2.5 and 3.0. For each field line a total of eight runs consisting of permutations of solar cycle (max or min), seasonal (winter or summer) and diurnal (day or night) boundary conditions were made. These boundary conditions were determined from Tables 2 to 4. Figure 2 contrasts two such runs for L = 2. Both are for daytime solar maximum conditions with the upper being for summer and the lower for winter. Each panel shows the H^+, He^+ and O^+ density variation along the magnetic field line as a function of altitude. Particularly noticeable is the enhanced summer O^+ densities and the reduced summer He^+ densities. These differences being associated with both the differences in boundary conditions, and with the enhanced winter He^+ being the winter He^+ bulge. For H^+ the boundary conditions are very similar in both winter and summer and yet a significantly enhanced summer profile is present. This is a result of the interaction between the three positive ions and the electron fluids through the ambipolar electric field. The higher temperature in summer can also result in a small enhancement of the summer profile. Figure 2 highlights a major difficulty in the diffusive equilibrium formulation, namely that the equatorial densities for the same field line (half summer, half winter) has different values depending upon from which hemisphere the solution is derived. This point will be addressed in detail in a later section.

In addition to the runs made for specific solar cycle, seasonal and diurnal conditions, a study was made of the sensitivity of the model to boundary conditions for the L=3 solar minimum-summer-daytime situation. The effect upon equatorial density and flux tube content of reasonable variations in either the ionospheric density boundary conditions or temperature profile were tested. The equatorial density was found to vary almost proportionally to the square root of the product of the O^+ and H^+ lower boundary density. This strong coupling between the light and heavy ions give a wide dynamic range of equatorial densities. In addition to this degree of freedom, the choice of temperature profile, either absolute or relative altitude distributions, yields a factor of two increase or decrease in the H^+ flux tube content. This factor can also be achieved by keeping the ionospheric and equatorial temperatures constant and changing the profile shape. Based upon these studies it appears that the diffusive equilibrium solution will give a wide range of variation due to the difficulty of supplying sufficiently specific boundary conditions, and hence the results to be presented should be viewed as mean trends bracketing extreme situations rather than specific values for the given set of geophysical parameters.

Figure 3 shows contour plots of the H^+ density for L = 1.15 to L = 3. Each panel shows a noon-midnight meridian cross-section of the earth and plasmasphere for the northern hemisphere, the dayside is on the left side of each panel and the seasonal condition is indicated by the shading on the earth. Dark shading indicated the region is in darkness. The upper two panels correspond to solar maximum conditions with summer and winter being the upper and lower of these two panels respectively. Solar minimum conditions are shown in the lower two panels with summer and winter again being shown by the upper and

lower of these two panels respectively. For each plasmaspheric condition the logarithm of the H^+ density along the L = 1.15, 1.5, 2.0, 2.5, 3.0 field lines were combined and contoured at 0.333 $\log_{10}$ (density) intervals.

For the eight cases shown in figure 3 the largest systematic variation is between corresponding solar maximum and solar minimum conditions. During solar maximum conditions (upper two panels) the densities are between two and ten times larger than at solar minimum, with the largest differences occurring at the greatest radial distances. Smaller density variations are observed between winter-summer or day-night, in both instances the variations are between factors of one and three. During solar maximum winter (top panel) the plasmaspheric density distributions are most uniform, with under two orders of magnitude density change; in contrast solar minimum shows over three orders of magnitude change. In general the H^+ density tends to decrease with radial distance and with latitude, although beyond a radial distance of about 2.5 Re the density increases slightly with latitude. These H^+ densities are not simply related to the H^+ boundary conditions. As shown by figure 2, the other ions, especially O^+, have a significant effect upon the equilibrium solution. Indeed the H^+ density shows proportionality to the square root of the O^+ boundary density.

Figure 4 shows solar maximum He^+ plasmaspheric density distributions for summer (top panel) and winter (lower panel). The densities are contoured at 0.333 intervals on a logarithmic scale, and densities are labelled in logarithmic values of the density in cm^{-3}. These two panels correspond to the H^+ top panels of figure 3. Comparing the H^+ and He^+ for summer conditions, top panel of figure 4 shows that He^+ has considerably lower densities, and a steeper radial rate of density decrease although the latitudinal variations

follow similar trends. In marked contrast the winter He^+ density, lower panel of figure 4, shows increasing value with increasing latitude, and winter densities an order of magnitude higher than the corresponding summer values. This winter-summer He^+ variation is sharply in contrast to that of H^+ and is due entirely to the high latitude winter helium bulge in the neutral atmosphere resulting in the enhanced winter He^+ ionospheric densities at high latitude.

From both figures 3 and 4 it is evident that not only is there a solar cycle dependence for the plasmaspheric density distribution but there are also seasonal and day-night dependencies. In order to study these latter two dependencies more quantitatively figure 5 shows the total ion flux tube content as a function of L value for the different conditions. The flux tube is assumed to have an area of 1 cm^2 at 675 km and extends to the equator, all three ions H^+, He^+ and O^+ are included in the total density. For solar maximum, left panel of figure 5, the flux tube content is almost independent of L value, however day contents are larger than night and summer contents larger than winter. Such a day-night trend also exists at solar minimum but the solar minimum conditions show a decrease of content with increasing L value.

The significantly reduced flux tube content for nighttime conditions compared to daytime conditions can, in part, be attributed to the choice of the boundary condition altitude at 675 km. At this altitude production and loss processes are still important for the light ions and consequently a day/night difference would be expected which would not necessarily reflect the change in flux tube content. Indeed the night time values must be treated as lower limits at best and probably reflect a boundary condition nighttime density maintained by plasma flow from the plasmasphere to the ionosphere. Of course such

a non-equilibrium flow situation severely constrains the validity of a diffusive equilibrium formulation should the diurnal modulation be indeed a factor of two to four as indicated by the day/night differences shown in figure 5.

A second area in which the diffusive equilibrium model is severely tested is that of winter/summer differences. Clearly our calculations which yield two sets of unequal densities at the equator are not self-consistent. In figure 5 it is evident that the most extreme summer-winter differences occur during the day, the time when the largest summer-winter ionospheric differences would be expected due to differences in production. Nighttime differences are smaller and should reflect differences in the maintenance processes for the ionosphere which if controlled by downward fluxes from the plasmasphere could be quite similar. These daytime summer-winter differences would for solstice conditions require more comprehensive interhemispheric models to resolve the equatorial differences. From the above discussion we expect that the diurnal ebb and flow of the flux tube contents associated with the diffusive equilibrium model and empirical boundary conditions would on the dayside take values sightly lower than those shown in figure 5 while at night they would be significantly higher than that shown although possibly still appreciably lower than during the day.

Comparison With Plasmaspheric Observations

Plasmaspheric parameters are observed by two quite different techniques, the first being the ground-based observation of whistler dispersion signatures and the second being an in-situ satellite measurement of a local parameter such as density, temperature or composition. The whistler technique uses the time dispersion of different frequency waves propagating in a whistler duct

(flux tube) from one ionosphere to the conjugate ionosphere. This dispersion signature when combined with a model of the flux tube density distribution yields parameters such as flux tube content or equatorial density, see Park (1972) for a detailed discussion on this technique. Park's analysis shows how a variety of different diffusive equilibrium models would produce an equivalent variety of flux tube contents and equatorial densities. His diffusive equilibrium models range from the classical variety with no allowance for flux tube divergence to "collisionless" which is almost identical to the Chiu et al (1979) and our own model which contain flux tube divergence. The major difference between these diffusive equilibrium models is that for the classical model the equatorial density is aproximately equal to the flux tube content/total volume whereas in the case of a "collisionless", divergent flux tube models the equatorial density is less than 20% of the average flux tube content. In-situ techniques of observing local parameters are unable to yield flux tube content or average flux tube density parameters but instead yield absolute local values.

1. Flux tube content

In figure 5 the range of model values for flux tube content are shown. For solar maximum (left panel) the content ranges between 2×10^{12} to 2×10^{13} for all flux tubes between L = 2 and L = 3. At solar minimum this range is considerably lower, from 6×10^{11} to 2×10^{12}, an order of magnitude lower. In both solar cycle cases shown in figure 5 there is a summer-winter and day-night variation, with the day-night variation being the larger of the two in general. These model values can be compared to the inferred values of Park (1974) and Park et al (1979) where whistler measurements have been analyzed using the classical diffusive equilibrium model. In the region between L = 2

and L = 3 Park (1974) obtained flux tube contents ranging from 4×10^{12} to 1.5×10^{13} for summer solar minimum conditions while in a more extensive study Park et al (1978) obtained values ranging from 4×10^{12} to 3×10^{13}. These values which cover a wide range of solar cycle, seasonal and diurnal condtions span the range of values for solar maximum shown in figure 5, however do not reflect the lower solar minimum values shown in figure 5. In fact the observed values should be increased by 15% to allow for our larger flux tube volume since our model is based at 675 km and not 1000 km as used by Park (1974) and Park et al (1978). The whistler observations show a marked seasonal variation and only a weak solar cycle variation based on the Park et al (1978) analysis. These observations were taken over the same time period the boundary conditions for this study were acquired. We have been unable to find measurements to agree with our predicted low values of total flux tube contents at solar minimum. Whistler measurements span solar minimum times, but consistently show higher flux tube contents than we predict. This suggests that either the diffusive equilibrium model is not applicable or that there or that there are difficulties in interpreting whistler measurements at low L-values and in a low density ionosphere.

2. Equatorial Density

Figure 6 shows a comparison of model (shaded areas) and observation of the equatorial density as a function of the L value (radial distance). For the model values the summer-winter extremes at both solar maximum and solar minimum are used to represent the bounds for the solar cycle shading in figure 6. The equatorial density curve shown as open circles joined by dashed lines are from Park (1974) under solar minimum conditions using whistler observations. Park et al (1978) show equatorial densities ranging from 5×10^2 to

10^3 cm^{-3} at L = 3. Hence the whistler equatorial densities span a range which lies above that inferred from our model. This discrepancy is perhaps not too surprising since the equatorial density is highly model dependent in the whistler analysis technique see Park (1972). For the whistler data referred to above the classical diffusive equilibrium model has been used and this would then infer a maximum value for equatorial density, whereas if a "collisionless" model were used values would be decreased by up to a factor of 5. The equatorial density data shown as crosses on a solid line in figure 6 represents upper limit of full flux tube inferred from in-situ observations of Chappell et al (1970) and Chappell (1974). This curve is taken from the OGO-5 satellite data in the vicinity of the 1800 local time bulge region where the densities are found to be somewhat higher than at other local times. This curve can be seen to be about a factor of 3 higher than the largest model values shown in figure 6. For L values greater than L = 3 this curve is lower than the whistler inferred value. The L-value dependence of the model closely parallels the $1/L^4$ decline observed by Chappell et al (1970), however the whistler data shows a considerably more gentle fall off. The final group of data points shown in figure 6 come from the GEOS-1 satellite (Johnson 1981) and represent upper limits on the cold H^+ (<1eV) equatorial density over the 1977 to 1978 period. These densities were obtained from two independent techniques, direct particle distribution measurements and measurement of the local upper hybrid frequency which yield plasma frequency. Although these observations were taken prior to sunspot maximum the solar EUV fluxes were high, averaging well over 100 on the F10.7 scale. Comparing all these values with the model clearly indicates an absence of the wide dynamic range inferred from the model based on low altitude boundary conditions. Indeed the range of variation indicated by the solar maximum shading would, if increased by a factor

of 2 to 3 in density, cover the observations.

3. Diurnal and Seasonal Variations

Both figures 5 and 6 show that the model results indicate a marked diurnal and seasonal variations. The seasonal variation is questionable since the model only solves for half a flux tube, leaving an ambiguity at the equator where the summer and winter flux tubes meet. This clearly indicates that under extreme seasonal conditions a flux tube could not be in diffusive equilibrium as modelled by our simple equations. To date only whistler observations have been able to accumulate enough data to infer either diurnal or seasonal variations. Park et al (1978) found a weak diurnal modulation at L = 3 where noon equatorial densities exceeded midnight densities by about 50%. This difference is clearly less than that inferred from our calculations. For L-vaues below 3 the whistler observations also show a seasonal modulation with December values of equatorial plasma density exceeding those in June by 50% (Park et al, 1978). This effect is not related to the model season variation which requires identical density ambiguities at the equator for both solstices. The fact that the whistler observations see a seasonal variation is itself indicative that diffusive equilibrium is not particularly applicable.

Summary

We have carried out a parametric study of boundary conditions applicable to diffusive equilibrium plasmaspheric models. These results were then compared with observed or inferred values of the equatorial density and flux tube content to yield the following conclusions.

1) The major, almost an order of magnitude, difference between solar maximum and solar minimum conditions obtained by the model based on empirical boundary conditions is not manifested in the observations of plasmaspheric parameters. A resolution of this problem would require new in-situ measurements at solar minimum conditions to verify that indeed negligible solar cycle variation is present in the plasmasphere; or more specific dynamic equilibrium model studies to understand how the highly solar cycle dependent topside ionosphere is decoupled from the plasmasphere.

2) Diffusive equilibrium models which solve for only one half of a field line, that is ionosphere to equator, introduce an ambiguous seasonal dependence. Since a strong seasonal dependence is observed in plasmaspheric observations it is highly indicative of a lack of diffusive equilibrium conditions and this must point to the existence of a dynamic plasma equilibrium.

3) Diurnal variations inferred from the model are somewhat higher than observed primarily due to the nighttime ionospheric boundary condition being lower than that which would best be associated with a diffusive equilibrium description of the plasmasphere.

4) Under solar maximum conditions the bulk properties of the plasmasphere can be described by a diffusive equilibrium formulation to an L-value of ≈ 3. A formulation using no magnetic flux tube divergence gives an upper limit while one using full flux tube divergence gives a lower limit.

5) Beyond $L \tilde{} 3$ diffusive equilibrium is rarely applicable due to the long time required to reach such a state (many days) in the presence of almost daily

storm activity. Under the few conditions when it would apply a diffusive equilibrium model which contains magnetic flux tube divergence would be the most appropriate.

Although many major advances in plasmaspheric theories have been made since the earliest uses of diffusive equilibrium to modelling the plasmasphere these advances have not resulted in a "global scale" replacement of the diffusive equilibrium plasmasphere model. The more recent models which include time dependent effects or dynamic equilibrium conditions would use exorbitantly large amounts of computer resources to have them incorporated into global plasmasphere descriptions. There are major requirements for a global plasmaspheric description, namely; interpretation of whistler observations; general inputs for magnetospheric problems; readily available method to deduce bulk parameters for plasmaspheric experiments; and a baseline against which high resolution in-situ observations can be compared in understanding other mechanisms also operating in the plasmasphere. Hence we feel that the use of diffusive equilibrium models although highly sensitive to boundary conditions can be used for global applications out to L~3 if they are used as indications of dynamic ranges in plasmaspheric parameters and not absolute unique values. Indeed the use of time dependent, dynamic equilibrium and diffusive equilibrium models in conjunction with in-situ observations at low and high altitudes (such as by the Dynamics Explorer satellites) is essential to understand the plasmasphere beyond our current global diffusive equilibrium standpoint.

Acknowledgement

This research was supported by NASA grant NAGW-77, NSF grant ATM-8217138 and Air Force Contract F-19628-83-K-001 to Utah State University.

TABLE 1

Observations Relevant to the Ion Density Boundary Conditions

Authors	Satellite	Comments
Taylor et al (1968)	OGO-2	solar minimum, latitudinal, composition.
Taylor et al (1970)	OGO-4	seasonal, light ions.
Brinton et al (1970)	Explorer 32	$O^+ - H^+$ transition altitude.
Taylor (1971)	OGO-4	Seasonal.
Taylor (1972)	OGO-6	Solar geomagnetic control.
Hoffman et al (1974)	ISIS 2	Solar maximum, day-night.
Breig and Hoffman (1975)	ISIS 2	Solar maximum, seasonal, compositon.
Raitt and Dorling (1976)	ESRO-4	Solar minimum, day-night.

TABLE 2a 675km Ion Density Boundary Conditions for $1.15 \leq L \leq 1.5$ (Region 1)

	SOLAR MAXIMUM		SOLAR MINIMUM	
	Day	Night	Day	Night
H^+ Summer	4×10^3 to 10^4	Same	3×10^3 to 5×10^3	Same
H^+ Winter	Same	Same	Same	Same
O^+ Summer	8×10^4 to 7×10^5 (2×10^5)	10^4	1×10^5	2×10^4
O^+ Winter	decreases with latitude from 7×10^5 at equator to 4×10^4 at 30° dip	factor of 20 to 40 lower than daytime	decreases with latitude from 2×10^5 at equator to 1×10^4 at 30° dip	Same
He^+ Summer	factor of 10 to 20 lower than H^+	Same	factor of 10 to 20 lower than H^+	Same
He^+ Winter	Same	Same	Same	Same

TABLE 2b 675km Ion Density Boundary Conditions for $1.5 \leq L \leq 3.0$ (Region 2)

	SOLAR MAXIMUM		SOLAR MINIMUM	
	Day	Night	Day	Night
H^+ Summer	4×10^3 (30° dip) to 2×10^3 (60° dip)*	Same	1.3×10^3 (30° dip) to 2.5×10^2 (60° dip)*	4×10^3 (30° dip) to 5×10^2 (60° dip)*
H^+ Winter	20% to 50% lower than O^+ winter day (7×10^3 to 7×10^2)	Same	1.6×10^3 (30° dip) to 4.0×10^2 (60° dip)*	3×10^3 (30° dip) to 2.5×10^2 (60° dip)*
O^+ Summer	8×10^4 to 10^5 constant with latitude	0.1 day value (10^4)	5 to 8 times greater than H^+ summer day (7×10^3)	O^+ 25% < H^+ at 30° dip $O^+ \geq H^+$ at 60° dip
O^+ Winter	10^4 (30° dip) to 10^3 (60° dip)*	0.1 day value	5 to 8 times greater than H^+ winter day (10^3)	O^+ 25% < H^+ at 30° dip $O^+ \geq H^+$ at 60° dip
He^+ Summer	= 0.05 H^+ value	Same	0.05 H^+	Same
He^+ Winter	Constant with latitude $He^+ = 0.5 H^+$ at 30° dip (3.5×10^3)	Same (3.0×10^3)	Constant with latitude $He^+ = 0.5 H^+$ at 30° dip (8×10^2)	Same

TABLE 3

Observations Relevant to the Plasma Temperature Boundary Conditions

Authors	Satellite	Comments
Brace et al (1967)	Explorer 22	Solar minimum, day-night, seasonal, ions.
Serbu and Maier (1970)	OGO-5	Solar maximum, day-night, ions.
Bezrukikh and Gringauz (1976)	PROGNOZ	Plasmasphere ions.
Rich et al (1979)	S3-3	Solar minimum, electrons.
Mahajon and Pandey (1979)	ISIS-1 and Explorer 22	Solar cycle, day-night, electrons.
Brace and Theis (1981)	AE-C, ISIS-1 and ISIS-2	Electrons.

TABLE 4a Plasma Temperature Profiles for $1.15 \leq L \leq 1.5$ (Region 1)

	SOLAR MAXIMUM		SOLAR MINIMUM	
	Day	Night	Day	Night
Plasma Temperature at 1000 km	3000° to 4000° ($\underline{3500}^{\circ}$)	$\underline{2000}^{\circ}$ to $\underline{2500}^{\circ}$ For L=1.15 For L=1.5	2000° to 2500° ($\underline{2300}^{\circ}$)	1000° to 1500° ($\underline{1200}^{\circ}$)
gradient to equator	increases by $\approx 1500^{\circ}$ to equator For L=1.5	= constant temperature	increases by $\approx 2700^{\circ}$ to equator For L=1.5	increases by $\approx 900^{\circ}$ to equator For L=1.5

TABLE 4b Plasma Temperature profiles for $1.5 \leq L \leq 3.0$ (Region 2)

	SOLAR MAXIMUM		SOLAR MINIMUM	
	Day	Night	Day	Night
Plasma Temperature at 1000km	30° dip same as Region 1 60° dip Tp=1.5 Tp at 30° dip	30° dip same as Region 1 60° dip Tp=1.5 Tp at 30° dip	30° dip same as Region 1 60° dip Tp=1.5 Tp at 30° dip	30° dip same as Region 1 60° dip Tp=1.5 Tp at 30° dip
Gradient to equator at 30° dip	From 3500° to 4700° at equator	From 2200° to 2200° at equator	Same as Region 1	Same as Region 1
Gradient to equator at 60° dip	to 4400° to $10,000^{\circ}$ at equator	From 2750° to 5000° at equator	From 2200° to $10,000^{\circ}$ at equator	From 1700° to 5000° at equator

References

Bailey, G. J., and R. J. Moffett, Temperatures in the polar wind, Planet. Space Sci., 22, 1193-1199, 1974.

Banks, P. M., Ion heating in thermal plasma flows, J. Geophys. Res., 78, 3186-3188, 1973.

Banks, P. M. and T. E. Holzer, The polar wind, J. Geophys. Res., 73, 6846-6854, 1968.

Banks, P. M., and T. E. Holzer, Features of plasma transport in the upper atmosphere, J. Geophys. Res., 74, 6304-6316, 1969a.

Banks, P. M. andT. E. Holzer, High-latitude plasma transport: The polar wind, J. Geophys. Res., 74, 6317-6332, 1969b.

Banks, P. M. and G. Kockarts, Aeronomy, (Part B), Academic Press, New York, 1973.

Banks, P. M., R. W. Schunk and W. J. Raitt, Temperature and density structure of thermal proton flows, J. Geophys. Res., 79, 4691-4702, 1974.

Banks, P. M., R. W. Schunk and W. J. Raitt, The topside ionosphere: A region of dynamic transition, Annl. Rev. Earth and Planet. Sci., 4, 381-440, 1976.

Bauer, S. J., Physics of Planetary Ionospheres, Springer-Verlay, Berlin- Heidelberd, 1973.

Bezrukikh, V. V. and K. I. Gringauz, The hot zone in the outer plasmasphere of the earth, J. Atmos. Terr. Phys., 38, 1085, 1976.

Brace, L. H., B. M. Reddy and H. G. Mayr, Global Behavior of the ionosphere at 1000-kilometer altitude, J. Geophys. Res., 72, 265-283, 1967.

Brace, L. H. and R. F. Theis, Global empirical models of ionospheric electron temperature in the upper F-region and plasmasphere based on in-situ measurements from the atmosphere explorer-C, ISIS-1 and ISIS-2 satellites, J. Atmos. Terr. Phys., 43, 1317, 1981.

Breig, E. L. and J. H. Hoffman, Variations in ion composition at middle and low latitudes from ISIS-2 satellite, J. Geophys. Res., 80, 2207, 1975.

Brinton, H. C., H. G. Mayr, R. A. Pickett and H. A. Taylor Jr., The effect of atmospheric winds on the $O^+ - H^+$ transition level, Space Research X (North-Holland, Amsterdam, 1970).

Chappell, C. R., Detached plasma regions in the magnetosphere, J. Geophys. Res., 79, 1861, 1974.

Chappell, C. R., K. K. Harris and G. W. Sharp, The morphology of the bulge region of the plasmasphere, J. Geophys. Res., 75, 3848, 1970.

Chiu, Y. T., J. G. Luhmann, B. K. Ching, and D. J. Boucher, An equilibrium model of plasmaspheric composition and density, J. Geophys. Res., 84, 909, 1979.

Hoffman, J. H., W. H. Dodson, C. R. Lippincott and H. D. Hammack, Initial ion composition resuls from the ISIS-2 satellite, J. Geophys. Res., 79, 4246, 1974.

Holzer, T. E., J. A. Fedder and P. M. Banks, A comparison of kinetic and hydrodynamic models of an expanding ion-exosphere, J. Geophys. Res., 76, 2453-2468, 1971.

Johnson, J. F. E., Magnetopsheric studies with suprathermal plasma analyses on the ESA GEOS satellites, Ph.D. Thesis, University of London, 1981.

Lemaire, J., O^+, H^+ and He^+ ion distributions in a new polar wind model, J. Atmos. Terr. Phys., 34, 1647-1658, 1972.

Lemaire, J. and M. Scherer, Model of the polar ion-exosphere, Planet. Space Sci., 18, 103-120, 1970.

Lemaire, J. and M. Scherer, Simple model for an ion-exosphere in an open magnetic field, Phys. Fluids, 14, 1683-1694, 1971.

Lemaire, J. and M. Scherer, Ion-exosphere with asymmetric velocity distribution, Phys. Fluids, 15, 760-766, 1972.

Lemaire, J., and M. Scherer, Kinetic models of the solar and polar winds, Rev. Geophys. Space Phys., 11, 427-468, 1973.

Mahajan, K. K. and V. K. Pandey, Solar activity chages in the electron temperature at 1000-km altitude from the Langmuir probe measurements on ISIS-1 and Explorer 22 satellites, J. Geophys. Res., 84, 5885, 1979.

Mange, P., The distribution of minor ions in electrostatic equilibrium in the high atmosphere, J. Geophys. Res., 65, 3833-3834, 1960.

Marubashi, K., Escape of the polar-ionosheric plasma into the magnetospheric tail, Rep. Ionos. Space Res. Japan, 24, 322-346, 1970.

Ottley, J. A. and R. W. Schunk, Density and temperature structure of helium ions in the topside polar ionosphere for subsonic outflows, J. Geophys. Res., 85, 4177-4190, 1980.

Park, C. G., Methods of determining electron concentrations in the magnetosphere from Nose Whistlers, Tech. Rep. 3454-1, Radioscience Lab., Stanford Electron. Lab., Stanford Univ., Stanford, Calif., 1972.

Park, C. G., Some features of plasma distribution in the plasmasphere deduced from Antarctic Whistlers, J. Geophys. Res., 79, 169, 1974.

Park, C. G., D. L. Carpenter and D. B. Wiggin, Electron density in the plasmasphere: Whistler data on solar cycle, annual and diurnal variations, J. Geophys. Res., 83, 3137, 1978.

Raitt, W. J. and E. B. Dorling, The global morphology of light ions measured by the ESRO-4 satellite, J. Atmos. Terr. Phys., 38, 1077-1083, 1976.

Raitt, W. J., R. W. Schunk and P. M. Banks, A comparison of the temperature and density structure in high and low speed thermal proton flows, Planet. Space Sci., 23, 1103-1117, 1975.

Raitt, W. J., R. W. Schunk and P. M. Banks, The influence of convection electric fields on thermal proton outflow from the ionosphere, Planet. Space Sci., 25, 291-301, 1977.

Raitt, W. J., R. W. Schunk and P. M. Banks, Helium ion outflow from the terrestrial ionosphere, Planet. Space Sci., 26, 255-268, 1978a.

Raitt, W. J., R. W. Schunk and P. M. Banks, Quantitative calculations of hel-

ium ion escape fluxes from the polar ionospheres, J. Geophys. Res., 83, 5617-5624, 1978b.

Rich, F. J., R. C. Sagalyn, and P. J. L. Wildman, Electron temperature profiles measured up to 8000 km by S3-3 in the late afternoon sector, J. Geophys. Res., 84, A4, 1328, 1979.

Schunk, R. W. and D. S. Watkins, Comparison of solutions to the thirteen-moment and standard transport equations for low speed thermal proton flows, Planet. Space Sci., 27, 433-444, 1979.

Schunk, R. W. and D. S. Watkins, Electron temperature anisotropy in the polar wind, J. Geophys. Res., 86, 91-102, 1981.

Schunk, R. W. and D. S. Watkins, Proton temperature anisotropy in the polar wind, J. Geophys. Res., 87, 171, 180, 1982.

Schunk, R. W., W. J. Raitt and A. F. Nagy, Effect of diffusion-thermal processes on the high-latitude topside ionosphere, Planet. Space Sci., 26, 189-191, 1978.

Serbu, G. P. and E. J. R. Maier, Observations from OGO-5 of the thermal ion density and temperature within the magnetosphere, J. Geophys. Res., 75, 6102, 1970.

Strobel, D. F. and E. J. Weber, Mathematical model of the polar wind, J. Geophys. Res., 77, 6864-6869, 1972.

Taylor, Jr., H. A., Evidence of solar geomagnetic seasonal control the topside ionosphere, Planet. Space Sci., 19, 77, 1971.

Taylor, Jr., H. A., Observed solar geomagnetic control of the ionosphere: implications for reference ionospheres, Space Research XII, 1275, 1972.

Taylor, Jr., H. A., H. C. Brinton, M. W. Pharo, III and N. K. Rahman, Thermal ions in the exosphere; Evidence of solar and geomagnetic control, J. Geophys. Res., 73, 5521, 1968.

Taylor, Jr., H. A., H. G. Mayr and H. C. Brinton, Observations of hydrogen and helium ions during a period of rising solar activity, Space Research X (North-Holland, Amsterdam, 1970).

Young, E. R., D. G. Torr and P. G. Richards, A flux preserving method of coupling first and second order equations to simulate the flow of plasma between the plasmasphere and ionosphere, J. Comp. Phys., 38, 141, 1980a.

Young, E. R., D. G. Torr, P. G. Richards and A. F. Nagy, A computer simulation of the midlatitude plasmasphere and ionosphere, Planet. Space Sci., 28, 881, 1980b.

Figure Captions

Figure 1 Plasma temperature at L = 2.5 for two extreme conditions, solar minimum night (dashed line) and solar maximum day (solid line) as a function of altitude from the ionospheric lower boundary to the equator.

Figure 2 Altitude profiles of H^+, He^+ and O^+ ion density for solar maximum-summer-daytime conditions (top panel) and for solar maximum-winter daytime conditions (lower panel). Both sets of profiles are for the L=2 magnetic field.

Figure 3 H^+ density contours for plasmaspheric field lines between L=1.15 and L=3. Each panel consists of a daytime (left half) and nighttime (right half) plasmaspheric cross-section. The density contours are at intervals of 0.333 on a logarithmic scale and are labelled in $\log_{10}(cm^{-3})$. The top two panels are for solar maximum summer (upper) and winter (lower) conditions while the bottom two panels are for solar minimum summer (upper) and winter (lower) conditions.

Figure 4 He^+ density contours for plasmaspheric field lines between L=1.15 and L=3. The upper panel being for solar maximum summer conditions while the lower is for solar maximum winter conditions. The format and contour intervals are the same as for figure 3.

Figure 5 Total ion flux tube content from the ionosphere to the equator for solar maximum (left panel) and solar minimum (right panel) as a function of the dipole L value. In each panel the seasonal summer (S) and winter (W) variations are shown for both daytime and night.

This seasonal difference is highlighted by the crosshatching.

Figure 6 Equatorial density comparison between model solar cycle conditions and observations over the plasmasphere as a function of radial distance.

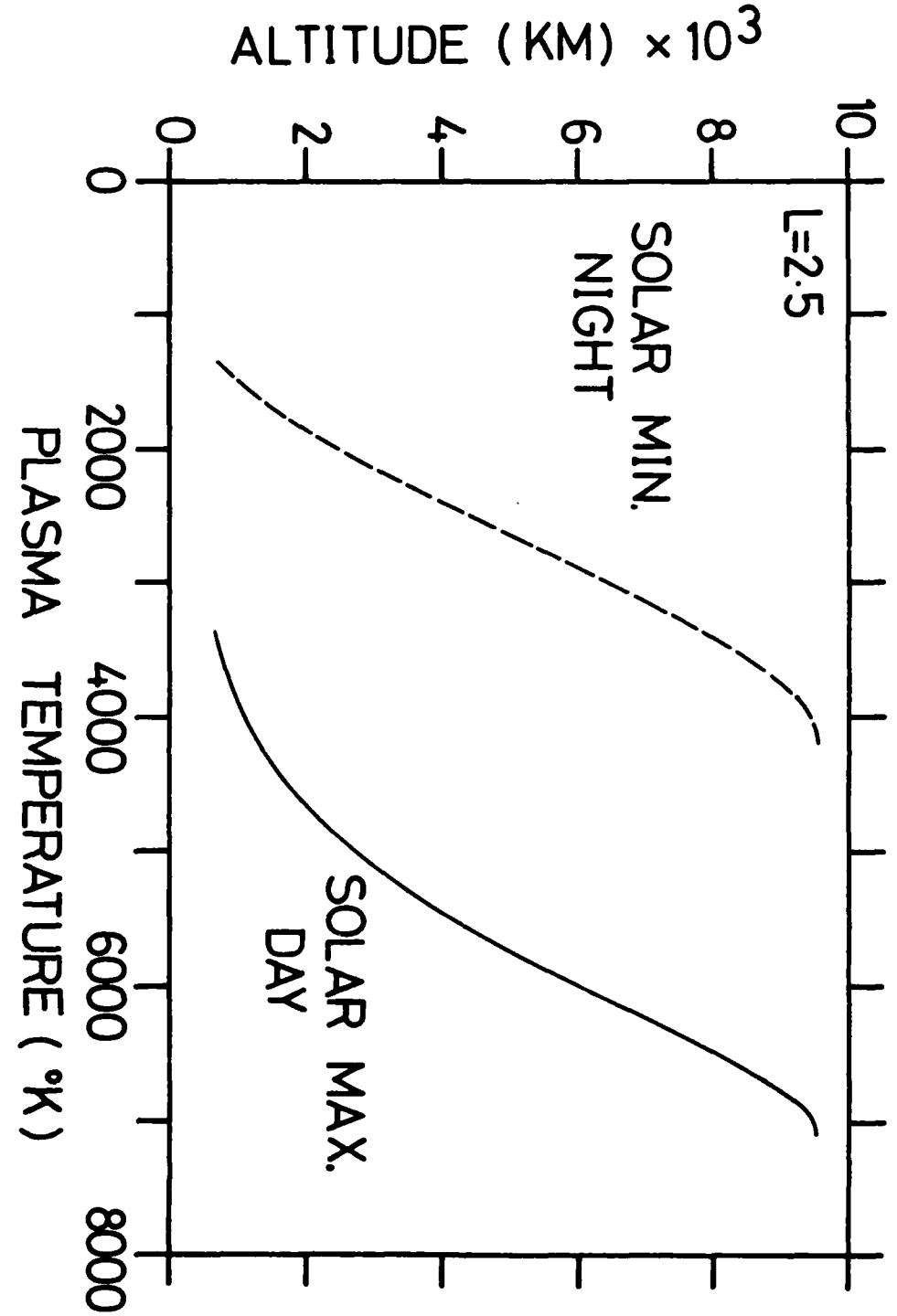
ALTITUDE (KM) ×10³
0
2
4
6
8
10
L=2.5
SOLAR MIN.
NIGHT
SOLAR MAX.
DAY
0
2000
4000
6000
8000
PLASMA TEMPERATURE (°K)

Figure 1

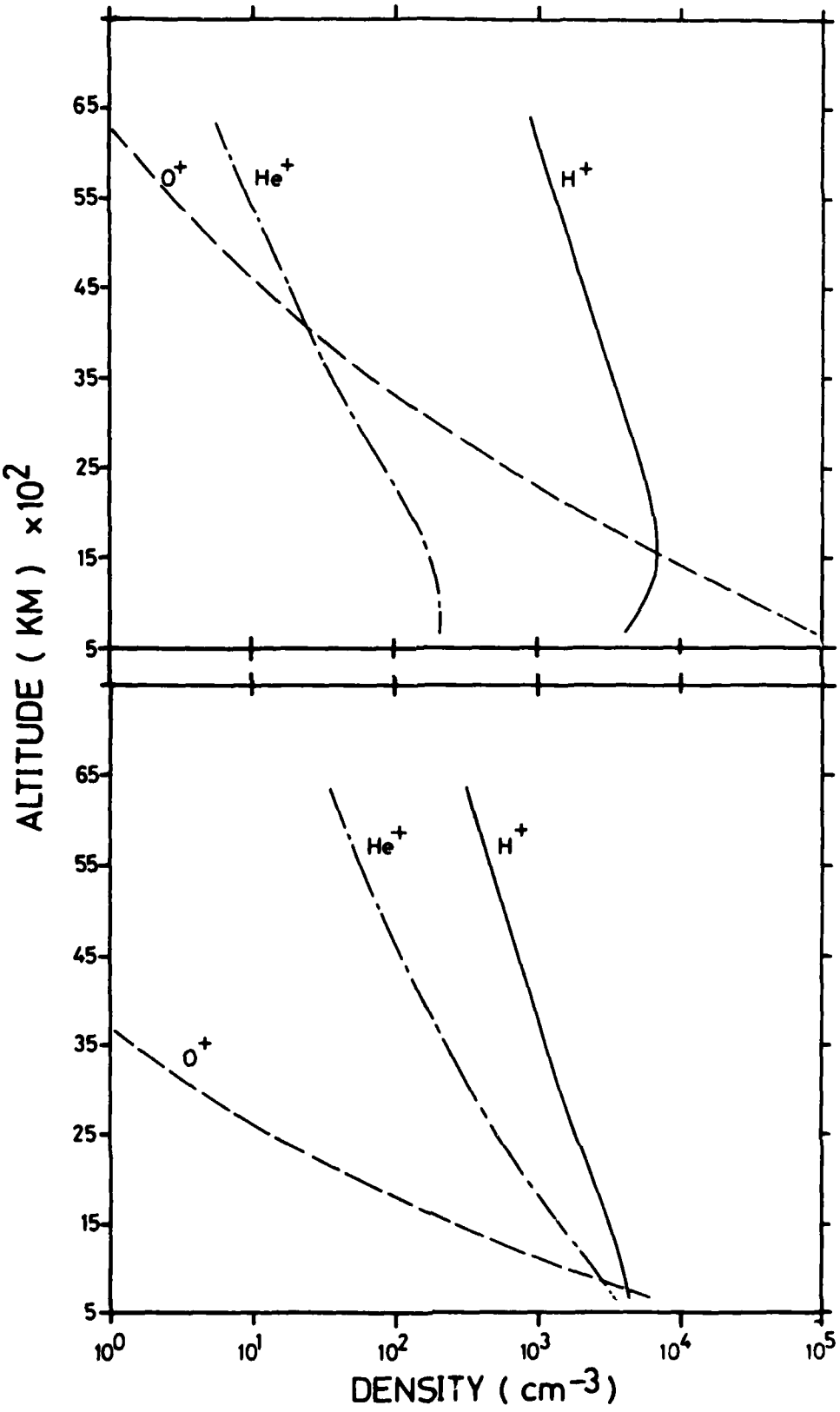
ALTITUDE (KM) x10²
65
55
45
35
25
15
5
O⁺
He⁺
H⁺
He⁺
H⁺
O⁺
10⁰
10¹
10²
10³
10⁴
10⁵
DENSITY (cm⁻³)

Figure 2

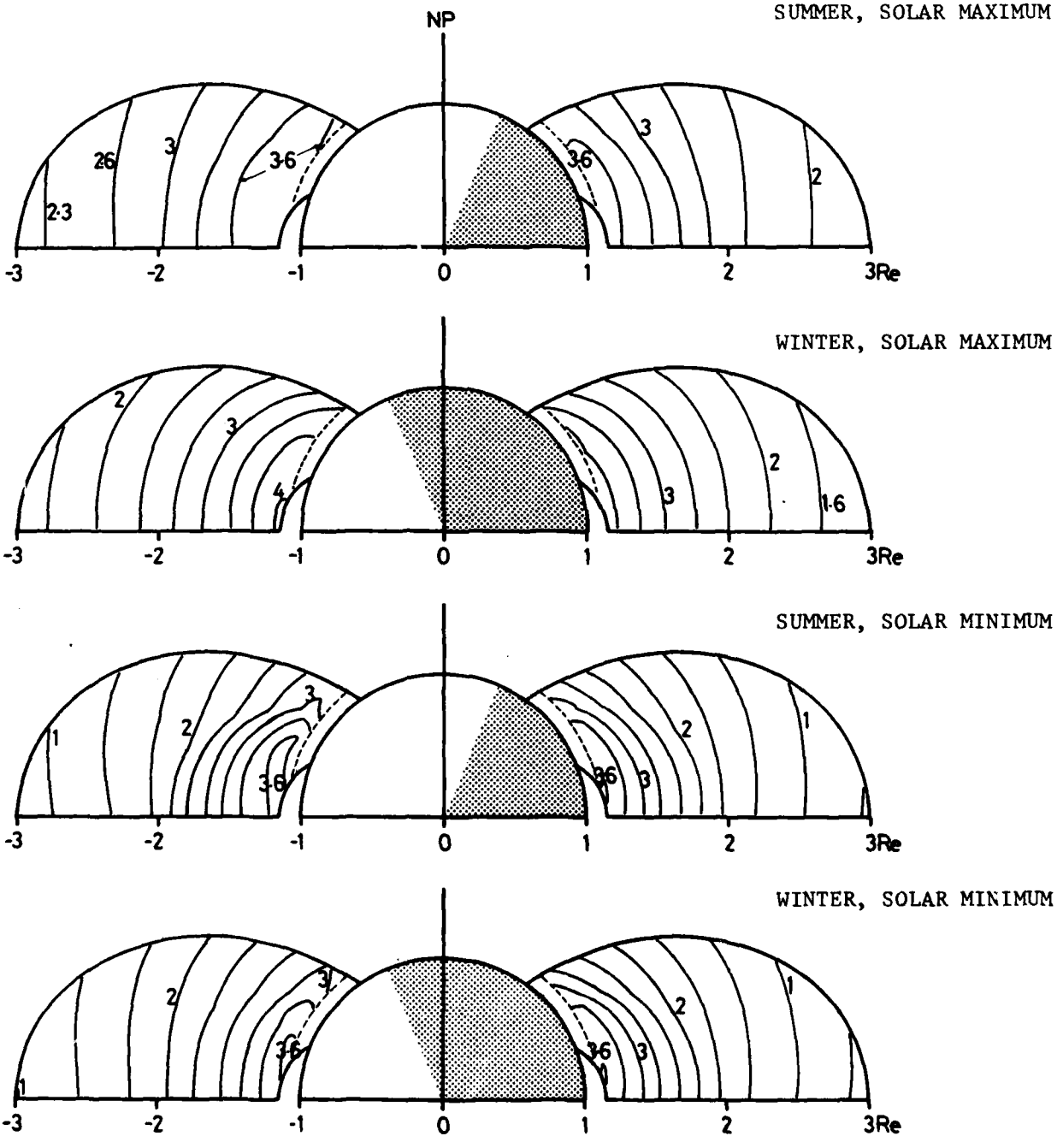
SUMMER, SOLAR MAXIMUM
NP
2·3
2·6
3
3·6
3·6
3
2
-3
-2
-1
0
1
2
3Re
WINTER, SOLAR MAXIMUM
2
3
4
3
2
1·6
SUMMER, SOLAR MINIMUM
1
2
3
3·6
3·6
3
2
1
WINTER, SOLAR MINIMUM
1
2
3
3·6
3·6
3
2
1

Figure 3

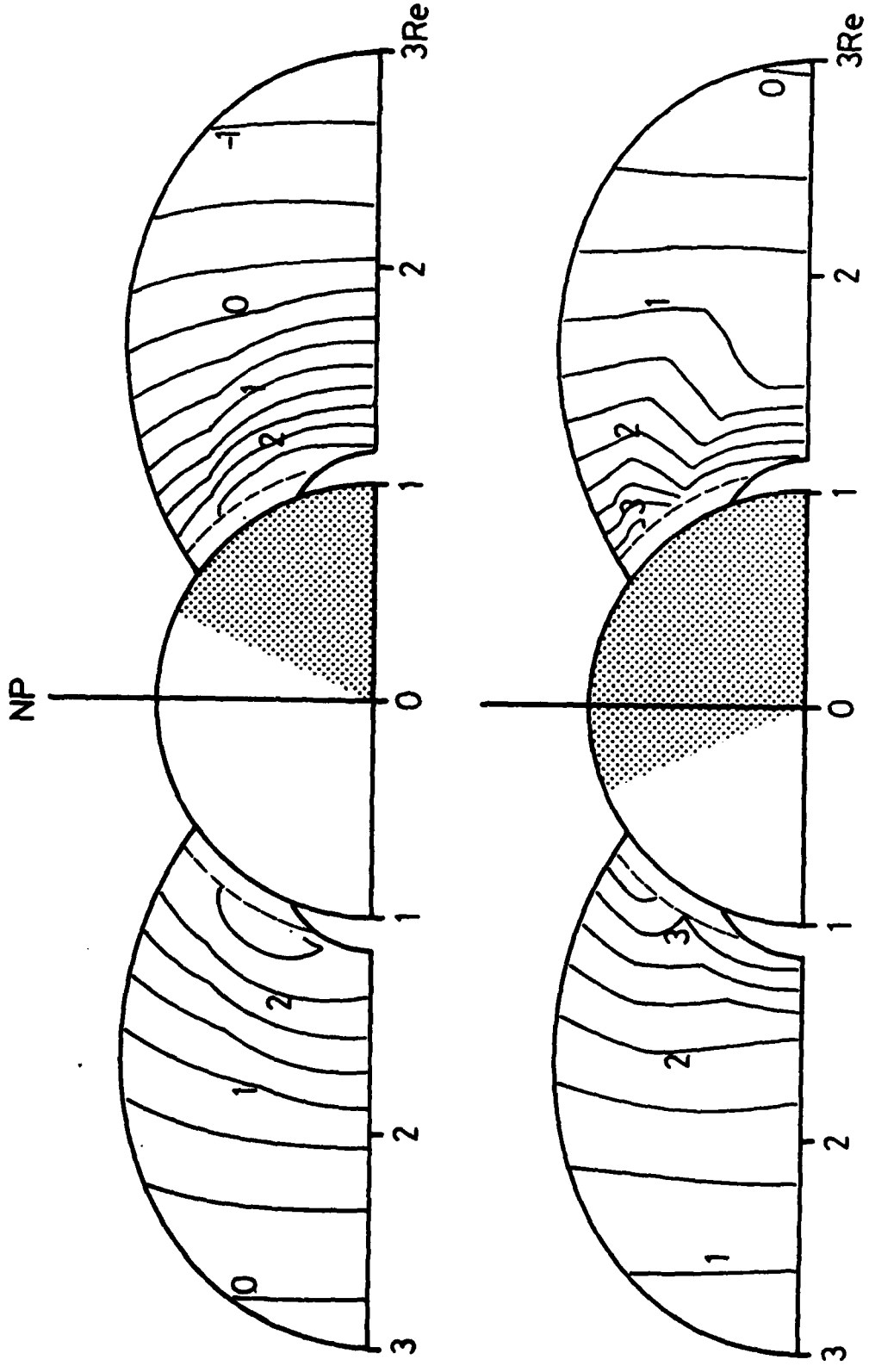

Figure 4

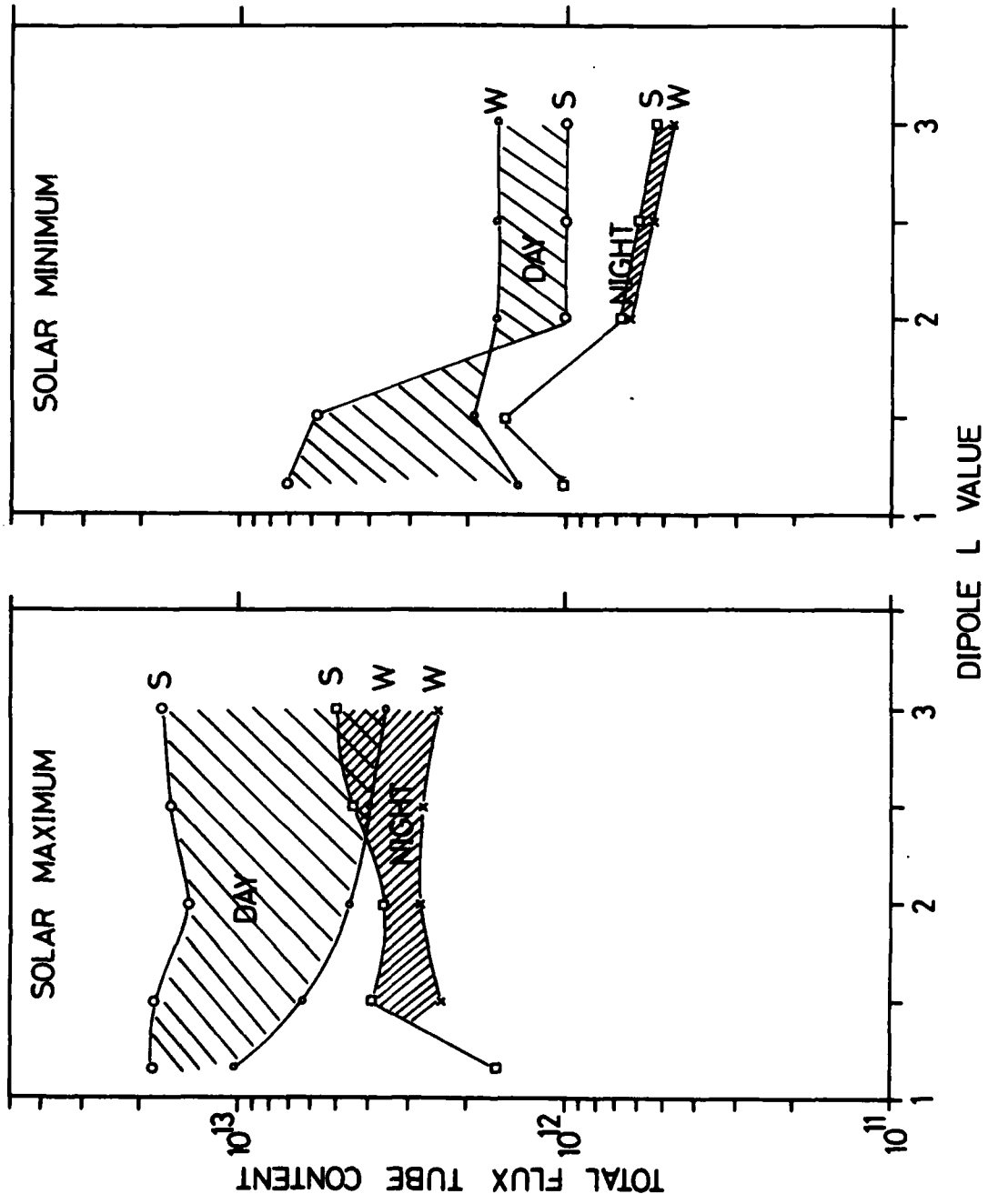
SOLAR MINIMUM
SOLAR MAXIMUM
DAY
NIGHT
S
W
TOTAL FLUX TUBE CONTENT
DIPOLE L VALUE

Figure 5

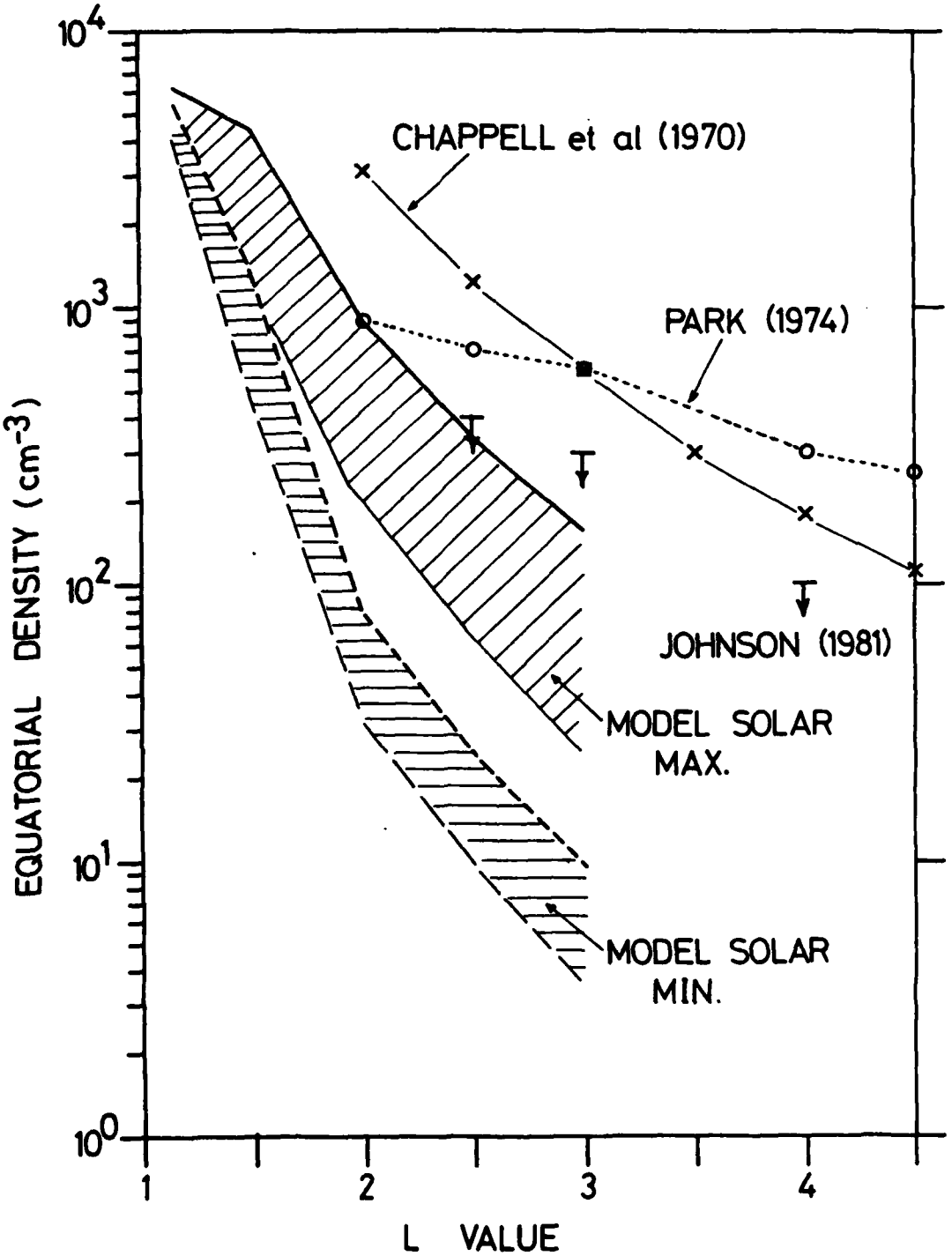
10^4
10^3
10^2
10^1
10^0
EQUATORIAL DENSITY (cm^{-3})
CHAPPELL et al (1970)
PARK (1974)
JOHNSON (1981)
MODEL SOLAR MAX.
MODEL SOLAR MIN.
1
2
3
4
L VALUE

Figure 6

END

FILMED

10-83

DTIC